PAPER

Improved thermal properties of polydimethylsiloxane by copolymerization and thiol–ene crosslinking of 2-pyrone-4,6-dicarboxylic acid moiety†

Takahiro Shimura,‡[a] Yijie Jin,‡[a] Keiichi Kubyama, [ID][a] Takuma Araki,[b] Naofumi Kamimura, [ID][c] Eiji Masai, [ID][c] Masaya Nakamura[b] and Tsuyoshi Michinobu [ID] *[a]

Recent environmental issues, such as global warming and climate change, have prompted a shift from petroleum-derived polymers to biomass polymers. We have developed new lignin-derived biomass polymers based on 2-pyrone-4,6-dicarboxylic acid (PDC), a metabolic intermediate of lignin. In previous studies, various polymers have been synthesized using PDC. Many of them showed strong adhesion to metal surfaces and biodegradability. On the other hand, despite the quasi-aromatic ring structure of PDC, its heat resistance remained unresolved. In this study, a diallyl PDC derivative was synthesized and copolymerized with polydimethylsiloxane (PDMS) by Pt-catalyzed hydrosilylation. The resulting polymers were further cross-linked using the PDC ring as the cross-linking point by using thiol–ene click chemistry. It was found that the heat resistance of PDMS was significantly improved by polymerization and cross-linking. By using biomass-based PDC, silicone rubber with low environmental impact, excellent heat resistance, and mechanical strength was successfully developed.

Introduction

To solve recent environmental issues, such as global warming and climate change, a shift from petroleum-derived polymers to biomass-based polymers has been desired.[1–5] Lignin is one of the most promising aromatic carbon resources with a three-dimensional reticular structure, while it has not been effectively used as a fine chemical in society.[6–10] Our previous study revealed that lignin can be converted to mixtures of low molecular weight aromatic ring fractions, which are then fermented by microorganisms to produce 2-pyrone-4,6-dicarboxylic acid (PDC) on a large scale using engineered *Pseudomonas putida* strains.[11] PDC consists of a polar pseudo-aromatic pyrone ring with two carboxyl groups, which can be condensed with diols

to synthesize various PDC-based polymers with good metal adhesion and mechanical properties.[12–21] However, heat resistance remained an unresolved issue because of the thermally degradable pyrone ring of PDC. For example, industrial poly(ethylene terephthalate) (PET) is synthesized by bulk polycondensation at >250 °C. In contrast, the previously reported PDC polyesters were not stable at such high temperatures. As biomass-based (pseudo)aromatic carbon resources are rare, it is desired to develop thermally stable biomass-based polymers and materials.

Silicone rubber (SR) is a class of elastomeric materials formed by cross-linking reaction with linear polysiloxane as the base material and exhibits excellent processability and elasticity in the broad operational temperature range.[22,23] In addition, since SR possesses superior resistance to high-energy particles, electronic irradiation, ultraviolet, ozone, aging, and other external stimuli, it is widely used in the fields of aerospace, machining, biomedical, *etc*.[24,25] Due to the tailored chemical and materials properties, we anticipated that SR would become a good platform to study the effect of the PDC unit on the heat resistance properties of SR.

In this study, diallyl PDC was synthesized and copolymerized with polydimethylsiloxane (PDMS), a heat-resistant silicone. Hydrosilane (H-SiR$_3$) is a relatively inert compound but readily undergoes addition to unsaturated bonds in the pres-

[a]Department of Materials Science and Engineering, Institute of Science Tokyo, 2-12-1 Ookayama, Meguro-ku, Tokyo 152-8552, Japan.
E-mail: michinobu.t.aa@m.titech.ac.jp
[b]Department of Forest Resource Chemistry, Forestry and Forest Products Research Institute, Tsukuba 305-8687, Japan
[c]Department of Materials Science and Bioengineering, Nagaoka University of Technology, Nagaoka 940-2188, Japan

‡These authors contributed equally.

ence of transition metal catalysts, such as Pt catalysts, which enables polymerization between diallyl PDC and PDMS.[26,27] The resulting polymers were further cross-linked using the PDC ring as the crosslinking point by using thiol–ene click chemistry to yield highly heat-resistant SRs, and their thermal and mechanical properties were fully characterized. Thermogravimetric analysis (TGA) of neat PDC powder suggested the onset decomposition temperature of 215 °C even under inert atmosphere.[28] However, it was surprisingly found that the PDC unit is thermally stable more than 400 °C under the same conditions when it was copolymerized and surrounded by hydrophobic PDMS. With this finding, PDC will be used in wider areas, especially being promising for heat-resistant polymers focused on low environmental impact.

Experimental

Materials and methods

2-Pyrone-4,6-dicarboxylic acid (PDC) was prepared from vanillic acid using an engineered *P. putida* strain, as reported previously.[11] Allyl alcohol, *N,N'*-diisopropylcarbodiimide (DIC), 4-dimethylaminopyridine (DMAP), Karstedt catalyst (19.0–21.5% as Pt), 1,6-hexanedithiol, and 1,4-diazabicyclo [2.2.2]octane (DABCO) were purchased from Tokyo Kasei Kogyo Co., Ltd (Tokyo, Japan). Poly(dimethylsiloxane) (M_n ~580) (PDMS-580) and poly(dimethylsiloxane) (M_n ~17 500) (PDMS-17.5k) were purchased from Sigma-Aldrich, Co. (Missouri, USA). Poly(dimethylsiloxane) (M_n ~1100) (PDMS-1.1k) was purchased from Gelest Inc. (Glen Rock, PA). Sylgard 184 was purchased from Dow Inc. (Kanagawa, Japan). All reagents were used without further purification.

Measurements

Thermogravimetric analysis (TGA) and differential scanning calorimetry (DSC) measurements were recorded under nitrogen flow on a Rigaku (Tokyo, Japan) Thermoplus TG8120 and DSC8230, respectively, at a heating rate of 10 °C min^{-1}, from 20 °C to 1000 °C for TGA and from −100 °C to 400 °C for DSC. Nuclear magnetic resonance (^{1}H NMR and ^{13}C NMR) spectra were recorded on a JEOL (Tokyo, Japan) model 400YH spectrometer at 20 °C. All chemical shifts are reported in parts per million downfield from SiMe$_4$, using the solvent's residual signal as an internal reference. The resonance multiplicity was described as s (singlet), d (doublet), t (triplet), and m (multiplet). Fourier transform infrared (FT-IR) spectra were recorded on a JASCO (Tokyo, Japan) FT/IR-4200 spectrometer. Gel permeation chromatography (GPC) was measured at 40 °C using a JASCO HSS-1500 system with a refractive index (RI) detector. *N,N*-Dimethylformamide (DMF) with lithium bromide (5 mM) was used as the eluent at the flow rate of 0.6 mL min^{-1}. Strain–stress (S–S) curve of the rubber films and tensile lap shear strength measurements were measured at 23 ± 2 °C with a Shimadzu Co. (Tokyo, Japan) autograph AGS-10kNX STD, according to ISO 37:2017 and JIS K 6850-1994, respectively.

Young's moduli were estimated from the initial (less than 0.5% elongation) slopes of S–S curves.

Synthesis

Diallyl 2-pyrone-4,6-dicarboxylic acid (DAPDC): PDC (1.00 g, 5.43 mmol) and allyl alcohol (1.00 mL, 14.7 mmol) were placed in a two-necked round bottom flask and tetrahydrofuran (THF) (20 mL) was added under argon. After cooling to 0 °C, 4-dimethylaminopyridine (0.132 g, 1.08 mmol) and *N,N'*-diisopropylcarbodiimide (2.00 mL, 13.0 mmol) dissolved in THF (20 mL) were added to the mixture. After stirring for 30 min and removal of by-products and solvent by filtration and evaporation, respectively, the residue was dissolved in chloroform (50 mL) and washed with 0.05 M hydrochloric acid, DI water, and saturated aqueous NaCl solution. The organic layer was dried over MgSO$_4$. Evaporation of the solvents furnished a crude product, which was purified by column chromatography (SiO$_2$, chloroform/THF 20 : 1) and dried *in vacuo*, affording DAPDC (0.519 g, 36%) as a white solid.

^{1}H NMR (400 MHz, CDCl$_3$, 293 K): δ = 7.52 (d, J = 1.5 Hz, 1H), 7.16 (d, J = 1.3 Hz, 1H), 6.03–5.92 (m, 2H), 5.47–5.29 (m, 4H), 4.89–4.79 (m, 4H) ppm; IR (neat): ν = 3473, 3091, 3023, 2981, 2943, 2880, 1727, 1643, 1562, 1523, 1455, 1368, 1326, 1234, 1169, 1110, 979, 939, 865, 778, 758, 712, 664, 551 cm^{-1}.

P1, P2, P3: PDMS (for **P1**: PDMS-580: 2.30 mL, 3.80 mmol; for **P2**: PDMS-1.1k, 4.30 mL, 3.80 mmol; for **P3**: PDMS-17.5k: 13.8 mL, 0.759 mmol) was placed in a two-necked round bottom flask, and toluene (for **P1**: 20 mL; for **P2**: 40 mL; for **P3**: 60 mL) was added under nitrogen. After heating to 110 °C, DAPDC (for **P1**: 0.970 g, 3.68 mmol; for **P2**: 1.010 g, 3.83 mmol; for **P3**: 0.201 g, 0.761 mmol) dissolved in toluene (1.0 mL) was added to the mixture. A solution of Karstedt catalyst (19.0–21.5% as Pt) (for **P1**: 0.20 mL, 0.247 mmol; for **P2**: 0.15 mL, 0.185 mmol; for **P3**: 0.040 mL, 0.049 mmol) in toluene (0.4 mL) was added, and the mixture was stirred for 48 h. After precipitation into methanol twice, the crude product was re-dissolved in chloroform and treated with activated carbon. After filtration and evaporation, the products were dried *in vacuo*, yielding the corresponding polymers, **P1** (2.63 g, 88%), **P2** (2.86 g, 58%), **P3** (12.6 g, 83%), respectively, as brownish viscous liquids.

P1: ^{1}H NMR (400 MHz, CDCl$_3$, 293 K): δ = 7.51 (s, nH), 7.13 (s, nH), 4.34–4.28 (m, 2nH), 1.82–1.72 (m, 2nH), 1.39–1.30 (m, 2nH), 0.96–0.90 (m, 2nH), 0.61–0.46 (m, 4nH), 0.14–0.01 (m, 6nmH) ppm; IR (neat): ν = 2961, 2904, 1753, 1564, 1441, 1331, 1257, 1014, 861, 791, 760, 700, 669 cm^{-1}.

P2: ^{1}H NMR (400 MHz, CDCl$_3$, 293 K): δ = 7.51 (s, nH), 6.98 (s, nH), 3.75–3.67 (m, 4nH), 1.26–1.20 (m, 8nH), 0.13–0.01 (m, 6nmH) ppm; IR (neat): ν = 2960, 2916, 2871, 1730, 1644, 1482, 1455, 1433, 1391, 1363, 1314, 1258, 1233, 1158, 1083, 1014, 862, 794, 756, 702, 666 cm^{-1}.

P3: ^{1}H NMR (400 MHz, CDCl$_3$, 293 K): δ = 7.51 (s, nH), 6.98 (s, nH), 3.81–3.61 (m, 4nH), 1.91–1.78 (m, 2nH), 1.31–1.15 (m, 4nH), 0.97–0.90 (m, 2nH), 0.19–0.01 (m, 6nmH) ppm; IR

(neat): ν = 2962, 2905, 1716, 1411, 1257, 1079, 1011, 862, 791, 700, 685, 661, 616, 607, 594, 518, 506 cm^{-1}.

R1, R2, R3: A mixture of DAPDC-PDMS polymer (for **R1**: **P1** 1.03 g; for **R2**: **P2** 1.93 g; for **R3**: **P3** 1.91 g), 1,6-hexanedithiol (for **R1**: 378 μL, 2.53 mmol; for **R2**: 454 μL, 3.28 mmol; for **R3**: 140 μL, 1.01 mmol), 1,4-diazabicyclo[2.2.2]octane (for **R1**: 295 mg, 2.53 mmol; for **R2**: 352 mg, 3.28 mmol; for **R3**: 22 mg, 0.20 mmol), and THF (for **R1**: 3.0 mL; for **R2**: 2.0 mL, for **R3**: 10 mL) was sonicated and spread on a Teflon boat. The solution was placed in a heated desiccator at 70 °C under ambient atmosphere for the first 2 h to allow the solvent to slowly evaporate, followed by a slow vacuum to completely evaporate the solvent for 48 h. After the reaction, the products were dried *in vacuo* at 100 °C, yielding the corresponding rubber-like polymers, **R1** (0.976 g, 80%), **R2** (2.19 g, ~100%), **R3** (1.76 g, 92%), respectively, as brownish solids.

R1: IR (neat): ν = 2960, 2926, 2854, 1733, 1687, 1617, 1457, 1410, 1258, 1078, 1016, 861, 793, 700 cm^{-1}.

R2: IR (neat): ν = 2961, 2905, 1733, 1698, 1683, 1558, 1540, 1507, 1456, 1411, 1398, 1257, 1078, 1012, 862, 790, 719, 683, 669, 660, 617, 594 cm^{-1}.

R3: IR (neat): ν = 2962, 2907, 1456, 1411, 1257, 1080, 1011, 862, 791, 754, 700, 660 cm^{-1}.

Results and discussion

Synthesis and characterization

DAPDC and a series of PDMS with different molecular weights were subjected to polyaddition using a Karsted catalyst to yield the corresponding polymers **P1–P3** (Scheme 1). The catalyst amount was optimized for this polymerization. GPC charts suggested the molecular weight increase after polymerization, but the polydispersity index (PDI) significantly increased especially in the case of **P3** (Table 1). The ^{1}H NMR spectra of **P1–P3** were measured in CDCl$_3$ at 20 °C (Fig. S3–S5†). In the ^{1}H NMR spectra of **P1–P3**, two small single peaks at 7.1 ppm and 7.5 ppm, ascribed to the PDC pyrone ring, were commonly observed. This result suggests that the PDC moiety was inert under the polymerization conditions. The PDMS siloxane chain was detected as an intense peak at 0.07 ppm. A comparison of the peak areas of the pyrone ring and siloxane protons indicates that the PDC content in **P1–P3** decreases in the order of **P1** > **P2** > **P3**. This is consistent with the molecular weights of the raw material PDMS.

Linear PDC-PDMS copolymers **P1–P3** were further crosslinked with 1,6-hexanedithiol in THF using a thiol–ene click reaction (Scheme 2).[29–36] The two alkenes on the PDC ring were employed as a crosslinking point. In the presence of DABCO, the thiol–ene click reaction efficiently proceeded at 70 °C.[37] After removal of the solvent, the resulting polymers **R1–R3** were insoluble in any solvents and became silicone rubber (SR).

The chemical structures of the raw material PDMS and the resulting polymers **P1–P3** and **R1–R3** were further characterized by FT-IR. The FT-IR spectra of PDMS showed almost the same peaks except for the peak intensity of Si–H vibration (Fig. 1). This reflects the different molecular weights of PDMS. For a series of sharp peaks at 1300–2000 cm^{-1} and 3570–3790 cm^{-1} of **R2**, these may be due to the contamination of the test environment with gaseous water. PDC-PDMS copolymers **P1–P3** showed the absence of the terminal Si–H peak at 2130–2110 cm^{-1}, suggesting that the terminal silane reacted with the terminal alkene of DAPDC. In addition, the peak intensity of the pyrone ring at 1730 and 1630 cm^{-1} decreased in the order of **P1** > **P2** > **P3**, which reflects the PDC content in the polymers. The FT-IR spectra of **R1–R3** showed the peak positions similar to those of **P1–P3**. The peak intensity at around 1630 cm^{-1}, ascribed to the two alkenes of the pyrone ring, is slightly reduced after crosslinking, indicating the successful progress of the thiol–ene click reaction.

Thermal properties

The thermal stability of PDMS, the PDC-PDMS copolymers **P1–P3**, and the crosslinked rubber **R1–R3** was investigated by thermogravimetric analysis (TGA). It was clearly shown that the thermal stability of PDMS depends on the molecular weights (Table 2). The 5% weight loss temperatures ($T_{d5\%}$s) of PDMS-580, PDMS-1.1k, and PDMS-17.5k were 95, 150, and 370 °C, respectively. This fact indicates that the thermal decomposition of PDMS initiates at the polymer terminals.[38–40] The thermal decomposition of siloxane chains is caused by the exchange at adjacent siloxane bonds, resulting in the formation of cyclic low-molecular-weight siloxane oligomers. This usually occurs at the ends of the siloxane chains or near the ends where the degree of freedom is relatively high.

Table 1 Molecular weights of **P1**-**P3** estimated from GPC

	M_w	M_n	PDI
P1	2.5×10^3	2.0×10^3	1.25
P2	8.1×10^3	6.7×10^3	1.21
P3	3.9×10^6	4.5×10^5	8.67

Scheme 1 Polymerization of DAPDC and PDMS to yield the copolymers **P1–P3** (**P1** from PDMS (M_n = 580), **P2** from PDMS (M_n = 1100), and **P3** from PDMS (M_n = 11 750)).

Scheme 2 Crosslinking of **P1**–**P3** with 1,6-hexanedithiol to yield **R1**–**R3**, respectively.
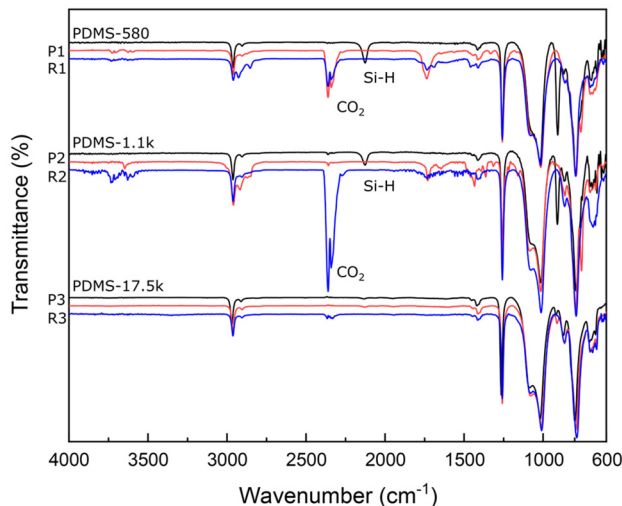
Fig. 1 FT-IR spectra of PDMS-580, PDMS-1.1k, PDMS17.5k, **P1**, **P2**, **P3**, **R1**, **R2**, and **R3**.

Table 2 Thermal properties of PDMS-580, PDMS-1.1k, PDMS17.5k, **P1**, **P2**, **P3**, **R1**, **R2**, and **R3**

	T_{d5} (°C)	T_m (°C)	ΔH_m (J g^{-1})
PDMS-580	95	−80	−14.6
PDMS-1.1k	150	−55	−43.8
PDMS-17.5k	370	−45	−39.0
P1	180	—	—
P2	250	—	—
P3	415	−40	−27.3
R1	185	—	—
R2	310	—	—
R3	430	−40	−34.3

Noticeably, the thermal stability of the polymers was significantly improved by copolymerization with PDC and further thiol–ene crosslinking (Table 2 and Fig. 2). Copolymerization with PDC was indeed an effective way of increasing molecular weights and thermal stability of PDMS, because it lowers the number of siloxane chain termini in the sample and suppresses the formation of cyclic siloxanes. Thus, the T_{d5} of **P1**–**P3** increased to 180, 250, and 415 °C, respectively. The TGA of DAPDC (comonomer of PDMS) suggested a well-defined weight decrease at about 200 °C, which is due to the decomposition of the pyrone ring. However, it should be noted that the previous TGA measurements of PDC derivatives were performed on an Al container and the pyrone ring reacts with an Al surface upon heating. Thus, the inherent thermal stability

of the PDC moiety has not yet been explored. In this study, the PDC units were surrounded by hydrophobic siloxane chains and were likely not in contact with the Al surface. This effect was most significant for **P3** among the three polymers. All these results suggest that the pyrone ring of PDC was intrinsically thermally stable above 400 °C if the ambient environment is properly prepared. Moreover, the crosslinking of **P1**–**P3** with 1,6-hexanedithiol further improved the thermal stability. The T_{d5} values of **R1**–**R3** were 185, 310, and 430 °C, respectively. This agrees with the general understanding that crosslinked resins are more thermally stable than the corresponding linear polymers.[41,42]

Differential scanning calorimetry (DSC) measurements were performed to investigate the phase behavior of the produced polymers. Unfortunately, due to the limitation of our instrument, the glass transition temperature of PDMS, typically observed around −120 °C, could not be evaluated. However, cooling PDMS to around −100 °C formed crystallization nuclei, and the subsequent heating produced exothermic peaks in the range from −80 to −40 °C, which are ascribed to the melting of crystals. Similar to the T_{d5} values, the melting point (T_m) of PDMS also depends on the molecular weights. PDMS-580 displayed a T_m of −80 °C, while the T_m gradually increased with the increasing molecular weights (−55 °C for PDMS-1.1k and −45 °C for PDMS-17.5k) (Fig. S6†). The melting enthalpy (ΔH_m) trend is almost consistent with this order (Table 2). Note that PDMS-1.1k and PDMS-17.5k displayed a weaker peak at higher temperatures (*ca.* −40 °C for PDMS-1.1k and *ca.* −35 °C for PDMS-17.5k), but this is due to the large supercooling.[43] Unlike PDMS, **P1** and **P2** showed no crystallization and melting peaks in the temperature range of −100 to 150 °C (Fig. S6†). On the other hand, **P3** exhibited a set of broader melting peaks in a similar temperature range to PDMS-17.5k. These results suggest that the introduction of the asymmetric PDC structure significantly lowered the crystallinity of PDMS. DSC of the crosslinked polymers was also measured. Similar to **P1** and **P2**, **R1** and **R2** displayed no crystallization and melting peaks. Interestingly, the melting points of **R3** were almost the same as those of **P3**, and the ΔH_m, calculated from the area of the melting peaks, slightly increased compared to **P3**. This result suggests that despite the crosslinked structure of **R3**, there is still sufficient intermolecular interaction between the siloxane chains.

Mechanical properties

The self-standing films of rubber-like materials **R1** and **R2** were prepared on a Teflon boat by crosslinking at 100 °C *in*

Fig. 2 TGA curves of (a) PDMS-580, **P1**, and **R1**; (b) PDMS-1.1k, **P2**, and **R2**; (c) PDMS-17.5k, **P3**, and **R3** at the heating rate of 10 °C min^{-1} under flowing nitrogen.

vacuo. The film thickness was controlled to be about 1.0 mm ± 0.1 mm. The films were then cut into dumbbell-shaped pieces and were subjected to the strain–stress (S–S) analysis at 23 ± 2 °C according to ISO 37:2017 (Fig. S7†). The narrow portion (10 mm ± 0.5 mm) of dumbbell-shaped pieces was the testing area. In addition, Sylgard 184, a commercial silicone rubber material, was employed as a control sample by curing it on a Teflon boat and was subjected to the same measurements.

The mechanical properties of PDMS also depend on the molecular weights. **R3** with the highest PDMS molecular weight was thus anticipated to show excellent mechanical properties. However, unfortunately, **R3** was not measured because it was difficult to cut out a dumbbell piece because of its adhesion to a Teflon boat and strong self-adhesion even when peeled off from a Teflon boat. The fracture strain, fracture stress, and Young's modulus, calculated from the S–S curve, are summarized in Table 3. Compared to Sylgard, **R1** has a lower fracture strain, but a higher fracture stress and Young's modulus. On the other hand, all the values of **R2** were lower than those of Sylgard, although the fracture strain was higher than **R1**. These results indicated that **R1** is a brittle but hard rubber material, while **R2** is a softer and easier-to-stretch rubber material. This difference is mainly due to the molecular weight of PDMS. Accordingly, the highly flexible characteristic of SR is more strongly reflected in **R2**. Although **R3** was not measured this time, it was the softest among **R1**–**R3** and stretched with a slight force. The viscosity of the linear siloxane reagent in Sylgard 184 before curing was close to that of PDMS-17.5k. Therefore, the molecular weight of the linear siloxane employed in Sylgard 184 is equivalent to PDMS-17.5k, and if the test species were successfully prepared, **R3** would exhibit mechanical properties comparable to those of Sylgard.

Adhesive properties

It has been demonstrated that PDC-containing polymers strongly adhere to metals, especially Al, Fe, and SUS plates.[44] The adhesion mechanism is based on the covalent bond formation between the metal surface and pyrone ring. In other words, the pyrone ring of the PDC unit was destroyed by the adhesion to metal surfaces. In order to gain insight into the presence or absence of PDC units in the crosslinked polymers, tensile lap shear strength measurements were performed according to JIS K 6850-1994 for measurements of adhesive properties. The size of the metal plate pieces (Al) used for the adhesion measurements was 25.0 mm × 100.0 mm × 1.6 mm. The surface of Al plates was washed under sonication with a series of solvents, and they were then treated with a Technovision Inc. (Saitama, Japan) UV-O$_3$ Cleaner UV-208 for 600 s. Approximately 50 mg of samples were cast on the Al plate surface. A set of two plates was placed in contact with each other by hot pressing at 10 MPa and cured for one hour under vacuum. The adhesive strengths were calculated as the failure force divided by adhesive area (25.00 ± 1.00 mm × 10.00 ± 1.00 mm).

Adhesion measurements were conducted on samples **P2**, **P3**, **R2** and **R3**. **P1** and **R1** were not tested because their decomposition temperatures were below 200 °C. However, **P2** and **R2** did not show adhesion at both 200 and 250 °C, as the specimens immediately peeled off after hot pressing. Therefore, only the **P3** and **R3** sets showed meaningful results. As summarized in Table 4, **P3** exhibited stronger adhesion of 5.45 and 5.78 kPa when pressed at 200 and 250 °C, respectively. The higher hot-press temperature was more effective due

Table 3 Mechanical properties pf **R1**, **R2** and Sylgard

	Fracture strain (mm mm^{-1})	Fracture stress (MPa)	Young's modulus (MPa)
Sylgard	1.27	0.24	0.33
R1	0.58	0.34	0.86
R2	0.64	0.07	0.16

Table 4 Tensile lap shear strengths (kPa) of **P3** and **R3** hot pressed at 200/250 °C for one hour according to JIS K 6850-1994

	Tensile lap-shear strength (kPa)	
Conditions	200 °C	250 °C
P3	5.45	5.78
R3	3.56	4.26

to the increase in the number of bonding sites with Al by ring-opening of PDC. The adhesive strengths of **R3** were lower than those of **P3**. The adhesive strengths of **R3** hot-pressed at 200 and 250 °C were 3.56 and 4.26 kPa, respectively. This result supports the occurrence of crosslinking at the PDC ring by thiol–ene click chemistry. This is also evidence of the adhesive mechanism between PDC polymers and metal surfaces.

Conclusions

By using biomass PDC and Si-based PDMS, SR materials with low environmental impact, excellent heat resistance, and mechanical strength were successfully synthesized. In this study, we have two significant findings. (1) The PDC unit exhibits thermal stability above 400 °C when surrounded by a hydrophobic, thermally inert environment. (2) The electron-deficient olefins of the PDC ring can be functionalized by thiol–ene click chemistry. These findings will be useful for future PDC studies pursuing biomass-derived engineering plastics and developing controlled crosslinking reactions.

Author contributions

Conceptualization, T.M.; investigation, T.S.; formal analysis, Y.J. and K.K.; resources, T.A., N.K., E.M., and M.N.; writing – original draft preparation, Y.J.; writing – review and editing, T.M.; funding acquisition, T.M. All authors have read and agreed to the published version of the manuscript.

Data availability

The data that support the findings of this study are available from the corresponding author upon reasonable request.

Conflicts of interest

There are no conflicts to declare.

Acknowledgements

References

1 R. Wei, G. von Haugwitz, L. Pfaff, J. Mican, C. P. S. Badenhorst, W. Liu, G. Weber, H. P. Austin, D. Bednar, J. Damborsky and U. T. Bornscheuer, *ACS Catal.*, 2022, **12**, 3382–3396.

2 B. Guo, S. R. Vanga, X. Lopez-Lorenzo, P. Saenz-Mendez, S. R. Ericsson, Y. Fang, X. Ye, K. Schriever, E. Bäckström, A. Biundo, R. A. Zubarev, I. Furó, M. Hakkarainen and P.-O. Syrén, *ACS Catal.*, 2022, **12**, 3397–3409.

3 G. Hayes, M. Laurel, D. MacKinnon, T. Zhao, H. A. Houck and C. R. Becer, *Chem. Rev.*, 2023, **123**, 2609–2734.

4 M. S. Kim, H. Chang, L. Zheng, Q. Yan, B. F. Pfleger, J. Klier, K. Nelson, E. L.-W. Majumder and G. W. Huber, *Chem. Rev.*, 2023, **123**, 9915–9939.

5 Y. Jiang, J. Li, D. Li, Y. Ma, S. Zhou, Y. Wang and D. Zhang, *Chem. Soc. Rev.*, 2024, **53**, 624–655.

6 W. Schutyser, T. Renders, S. V. D. Bosch, S.-F. Koelewijin, G. T. Beckham and B. F. Sels, *Chem. Soc. Rev.*, 2018, **47**, 852–908.

7 Q. Mei, X. Shen, H. Liu and B. Han, *Chin. Chem. Lett.*, 2018, **30**, 15–24.

8 H. Guo, Y. Zhao, J.-S. Chang and D.-J. Lee, *Bioresour. Technol.*, 2023, **384**, 129294.

9 F. F. Menezes, V. M. Nascimento, G. R. Gomes, G. J. M. Rocha, M. Strauss, T. L. Junqueira and C. Driemeier, *Fuel*, 2023, **342**, 127796.

10 A. Bleem, R. Kato, Z. A. Kellermyer, R. Katahira, M. Miyamoto, K. Niinuma, N. Kamimura, E. Masai and G. T. Beckham, *Cell Rep.*, 2023, **42**, 112847.

11 Y. Otsuka, T. Araki, Y. Suzuki, M. Nakamura, N. Kamimura and E. Masai, *Bioresour. Technol.*, 2023, **377**, 128956.

12 T. Michinobu, M. Hishida, M. Sato, Y. Katayama, E. Masai, M. Nakamura, Y. Otsuka, S. Ohara and K. Shigehara, *Polym. J.*, 2008, **40**, 68–75.

13 T. Michinobu, Y. Inazawa, K. Hiraki, Y. Katayama, E. Masai, M. Nakamura, S. Ohara and K. Shigehara, *Chem. Lett.*, 2008, **37**, 154–155.

14 T. Michinobu, M. Bito, M. Tanimura, Y. Katayama, E. Masai, M. Nakamura, Y. Otsuka, S. Ohara and K. Shigehara, *Polym. J.*, 2009, **41**, 843–848.

15 T. Michinobu, M. Bito, Y. Yamada, M. Tanimura, Y. Katayama, E. Masai, M. Nakamura, Y. Otsuka, S. Ohara and K. Shigehara, *Polym. J.*, 2009, **41**, 1111–1116.

16 T. Michinobu, M. Bito, M. Tanimura, Y. Katayama, E. Masai, M. Nakamura, Y. Otsuka, S. Ohara and K. Shigehara, *J. Macromol. Sci., Part A: Pure Appl.Chem.*, 2010, **47**, 564–570.

17 T. Michinobu, K. Hiraki, Y. Inazawa, Y. Katayama, E. Masai, M. Nakamura, S. Ohara and K. Shigehara, *Polym. J.*, 2011, **43**, 648–653.

18 Y. Cheng, K. Kuboyama, S. Akasaka, T. Araki, E. Masai, M. Nakamura and T. Michinobu, *Polym. Chem.*, 2022, **13**, 6589–6598.

19 Y. Jin, M. Joshi, T. Araki, N. Kamimura, E. Masai, M. Nakamura and T. Michinobu, *Polymers*, 2023, **15**, 1349.

20 H. Jia, K. Jimbo, K. Mayumi, T. Oda, T. Sawada, T. Serizawa, T. Araki, N. Kamimura, E. Masai, E. Togawa, M. Nakamura and T. Michinobu, *ACS Sustainable Chem. Eng.*, 2024, **12**, 501–511.

21 Y. Jin, T. Araki, N. Kamimura, E. Masai, M. Nakamura and T. Michinobu, *RSC Sustainability*, 2024, **2**, 1985–1993.

22 G. Wang, A. Li, W. Zhao, Z. Xu, Y. Ma, F. Zhang, Y. Zhang, J. Zhou and Q. He, *Adv. Mater. Interfaces*, 2021, **8**, 2001460.

23 M. Bont, C. Barry and S. Johnston, *Polym. Eng. Sci.*, 2021, **61**, 331–347.

24 D. Yang, W. Zhang and B. Jiang, *Ceram. Int.*, 2013, **39**, 1575–1581.

25 Z. Liu, Y. Huang, L. Yan, Y. M. Liang and H. Zou, *Prog. Org. Coat.*, 2022, **165**, 106773.

26 S. Luleburgaz, U. Tunca and H. Durmaz, *Polym. Chem.*, 2023, **14**, 2949–2957.

27 N. Yoshida, H. Zhu and M. Mitsuishi, *Polym. Chem.*, 2024, **15**, 1204–1211.

28 T. Michinoub, M. Bito, Y. Yamada, Y. Katayama, K. Noguchi, E. Masai, S. Ohara and K. Shigehara, *Bull. Chem. Soc. Jpn.*, 2007, **80**, 2436–2442.

29 C. E. Hoyle and C. N. Bowman, *Angew. Chem., Int. Ed.*, 2010, **49**, 1540–1573.

30 A. B. Lowe, *Polym. Chem.*, 2010, **1**, 17–36.

31 C. Resetco, B. Hendriks, N. Badi and F. Du Prez, *Mater. Horiz.*, 2017, **4**, 1041–1053.

32 M. Ahangarpour, I. Kavianinia, P. W. R. Harris and M. A. Brimble, *Chem. Soc. Rev.*, 2021, **50**, 898–944.

33 J. C. Worch and A. P. Dove, *Acc. Chem. Res.*, 2022, **55**, 2355–2369.

34 R. D. Murphy, R. V. Garcia, A. Heise and C. J. Hawker, *Prog. Polym. Sci.*, 2022, **124**, 101487.

35 X. Chen and T. Michinobu, *Macromol. Chem. Phys.*, 2022, **223**, 2100370.

36 S. Segawa, X. He and B. Z. Tang, *Luminescence*, 2024, **39**, e4619.

37 B. D. Fairbanks, D. M. Love and C. N. Bowman, *Macromol. Chem. Phys.*, 2017, **218**, 1700073.

38 A. Tasic, M. V. Pergal, M. Antić and V. V. Antic, *J. Serb. Chem. Soc.*, 2017, **82**, 1395–1416.

39 G. Camino, S. M. Lomakin and M. Lageard, *Polymer*, 2002, **43**, 2011–2015.

40 F. Chuang, H. Tsi, J. Chow, W. Tsen, Y. Shu and S. Jang, *Polym. Degrad. Stab.*, 2008, **93**, 1753–1761.

41 G. Tillet, B. Boutevin and B. Ameduri, *Prog. Polym. Sci.*, 2011, **36**, 191–217.

42 J. Huang and S. R. Turner, *Polym. Rev.*, 2018, **58**, 1–41.

43 P. A. Klonos, *Polymer*, 2018, **159**, 169–180.

44 M. Hishida, K. Shikinaka, Y. Katayama, S. Kajita, E. Masai, M. Nakamura, Y. Otsuka, S. Ohara and K. Shigehara, *Polym. J.*, 2009, **41**, 297–302.